Tellus (1992), *44A*, 133–154

Polar lows and arctic instability lows in the Bear Island region

By ERIK A. RASMUSSEN, *Geophysical Institute, University of Copenhagen, Haraldsgade 6, DK-2200 Copenhagen N, Denmark*, TORBEN S. PEDERSEN, *Danish Meteorological Institute, Lyngbyvej 100, DK-2100 Copenhagen E, Denmark*, LEIF T. PEDERSEN, *Electromagnetic Institute, Technical University of Denmark, DK-2800 Lyngby, Denmark* and JOHN TURNER, *British Antarctic Survey, High Cross Madingley Road, Cambridge CB3 0ET, England*

(Manuscript received 19 November 1990; in final form 25 October 1991)

ABSTRACT

The study of the "polar low episode" over the northern parts of the Norwegian Sea and the Barents Sea from 12 December 1982 to 16 December 1982 is continued. The role of baroclinic instability in the initial formation of a polar low near the ice edge is considered, including a discussion based on a diagnostic IPV analysis. During the polar low episode, circulations develop on different horizontal scales including true mesoscale phenomena. The mesoscale circulations have the character of symmetric vortices of a much smaller horizontal scale, ~100 km, than normally associated with polar lows. Although, during their initial formation, these circulations may be modulated by baroclinic instability associated with a shallow arctic frontal zone, they are predominantly convectively driven. The term "arctic instability lows" is suggested for these disturbances in order to distinguish them from the more "normal" polar lows. The polar low formations take place within a large synoptic scale cold dome. The importance of this cold dome as well of cold domes in general for polar low formations is briefly discussed.

1. Introduction

Research for more than 10 years has verified the existence of a variety of types of polar lows (e.g., Rasmussen and Lystad, 1987). The "Bear Island polar lows" which develop in the region between Svalbard and northern Norway are some of the most spectacular polar lows*. In an earlier study, (Rasmussen 1985, in the following referred to as R85) some aspects of the formation of a Bear Island polar low were discussed with special emphasis on the upper-air conditions prior to developments at the surface. The formation of this low was the first in a series of polar low formations which took place in the same region over several days thus allowing it to be classified as a "polar low episode" or a "polar low outbreak" (Businger, 1985). The present paper may be considered an extension of R85, as some of the ideas mentioned briefly in R85 will be elaborated on.

The present study shows that the formation and structure of some polar lows is very complex. While the interaction between phenomena on different horizontal scales is not very well understood, it is clear that convection and baroclinic instability are both important. One important result of this study is that some polar lows are of an even smaller scale than hitherto recognized, about 100 km. These mesoscale disturbances, however, are embedded in a somewhat larger cyclonic circulation on the synoptic scale.

Using arguments based on the application of the quasi-geostrophic omega equation, Reed (1986) points out "that migratory, upper-level vorticity maxima can play an role in the development of polar lows over the Norwegian Sea, a region sometimes thought to be populated by a class of polar lows quite unlike the comma cloud." While we agree with Reed as to the role of the initial

* A polar low formed near Bear Island with a striking resemblance to a small hurricane is discussed in a paper by Nordeng and Rasmussen (1992).

baroclinic forcing through differential vorticity advection, we claim, that the Norwegian Sea-region indeed seems "to be populated" by at least some polar lows different from the type of storm normally associated with comma clouds. Examples of such will be discussed in Section 3.

Recently, the widespread interest in "IPV thinking" has led to its application in diagnostic studies of observed cases of cyclogenesis. In Section 2, we show that prior to the surface development, an upper level IPV anomaly of fairly large horizontal scale could be observed advancing into the region where the polar low development subsequently took place. The use of the IPV concept highlights the importance of the "solitary" upper-level disturbance which triggers the surface polar low and provides a conceptual model which helps to understand and interpret the satellite images.

In Section 3 we discuss the "convective phase" of the polar low(s) development. In this phase, a tight mesoscale vortex is formed through a rapid spin-up of vorticity associated with the previously formed baroclinic low. This development in many ways resembles the formation of a subsynoptic/mesoscale vortex over the Mediterranean discussed by Rasmussen and Zick (1987). The first mesoscale vortex formed a little west of weather ship AMI (71.5° N, 19° E), and the center of the vortex subsequently passed very close to AMI. Surface observations taken during the passage make it possible to estimate the horizontal scale of the vortex and the maximum wind force. Later on another small scale vortex passed over Bear Island. The structure of this vortex will be discussed in Section 3. The use of passive microwave measurements in observing polar lows is also briefly considered in Section 3. Finally a summary and concluding remarks appear in Section 4.

2. The baroclinic phase (phase one)

In R85, it was shown that the Bear Island polar low originated from a small-scale upper-level cold core vortex whose origin could be traced eastward as far as Novaya Zemlya. An infrared satellite mosaic-picture composed from several successive orbits from around 1300 GMT 12 December 1982 shows the first polar low (A) in the incipient stage just west of Bear Island (Fig. 1). East of Scandinavia (seen in the middle of the picture) the two arrows marked B indicate a widespread cloud-deck associated with the polar front. Apart from the clouds associated with polar low A relatively few high clouds are seen over the arctic region north of 70° N. Fig. 1 illustrates in a striking way that some polar lows can develop far north of the main baroclinic zone, i.e., the polar front. The infrared satellite image from 1257 GMT 12 December 1982 from the NOAA-7 polar orbiting satellite shown in Fig. 2 gives a detailed view of the low and its surroundings. The eastern part of the relatively high clouds west of Bear Island form a comma with the comma-tail stretching in a southwesterly direction. The comma merges with another region of upper level clouds farther west. Extensive low-level cloud streets give evidence of the advection of cold air from the ice covered region between northern Svalbard and northeast Greenland. Closer to the polar low itself, cloud streets point to the very cold air that is streaming out from the ice edge stretching from west of Svalbard to Bear Island. As the low level disturbance developed close to the ice very cold air masses were drawn into the circulation and advected in a southerly direction. Subsequently a sharp arctic front with deep convection developed at the leading edge of the shallow cold air outbreak. At this time (12 GMT, 12 December) before the onset of deep convection, the ascent around the incipient polar low was dynamically forced, and both upper-level differential vorticity advection as well as low level thermal advection were likely to have been important. The radiosonde ascent from Bear Island 12 GMT, 12 December (R85, Fig. 9a) close to the time of the satellite image (Fig. 2) confirms that the clouds associated with the comma are due to stable ascent, and that free convection from the surface was very unlikely at this time. 14 h later, at 0250 GMT 13 December, the disturbance seen on Fig. 2 had developed into the impressive cloud spiral seen on Fig. 3. Very little development can be observed at the surface at that time from the conventional analysis, and it is a problem relevant to researchers and operational meteorologists alike, that the phenomenon seen on Fig. 3 does not fit very well into any of the conceptual models normally applied for developing cyclones.

The polar lows studied in this work all develop within the central and coldest region of a synoptic scale cold dome. During 12 and 13 December,

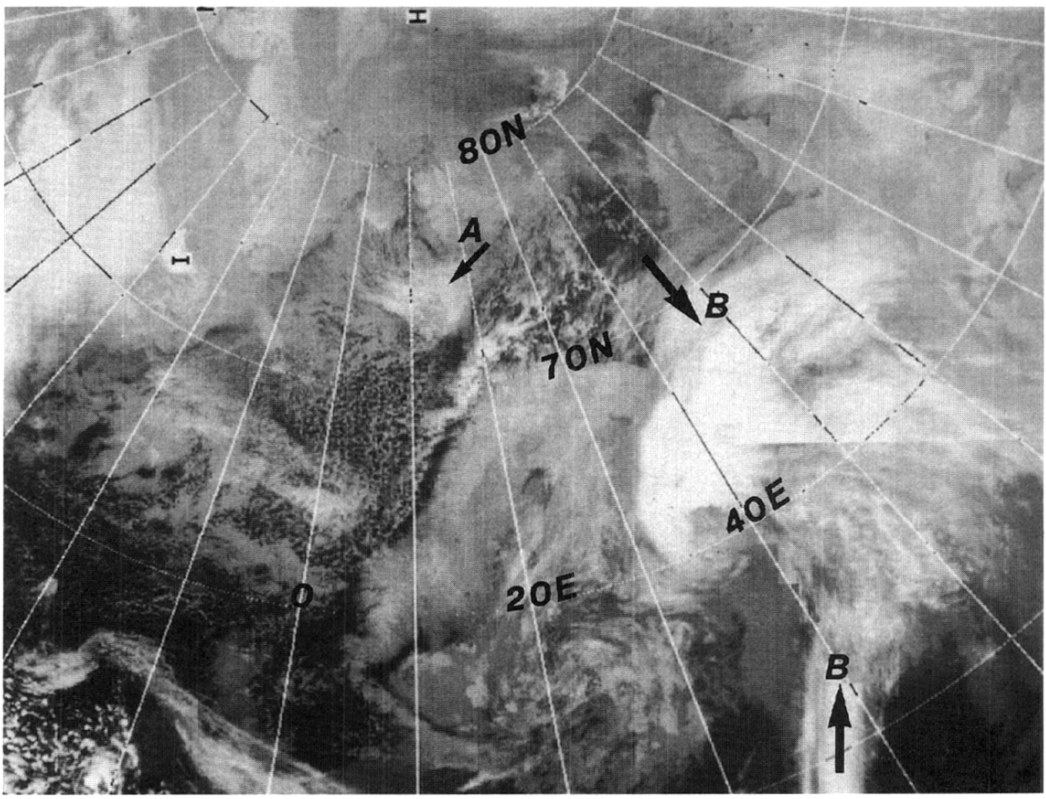

Fig. 1. NOAA-mosaic 12 December 1982. The arrow marked A shows the incipient polar low (around 1300 GMT) deep in the cold air mass. The arrows marked B indicate clouds belonging to the polar front. The Scandinavian Peninsula is seen in central part of the picture.

the center of the cold dome slowly moves in a southerly direction from Svalbard towards the region around North Cape as discussed in Subsection 3.3.

2.1. An IPV-description of the initial phase of the Bear Island polar low development

In many cases, the quasi-geostrophic omega-equation has proved to be a useful tool for understanding some phases/aspects of polar low developments as for example the role of initial baroclinic forcing through differential vorticity advection. However, a reliable, detailed analysis of the development by means of the omega-equation is not possible in this case, because of the small scales involved and the lack of data on these scales.

An alternative way to understand the dynamics of the developing polar low which partly overcome the difficulties mentioned above, is to apply the idea of potential vorticity (Eliassen and Kleinschmidt, 1957; Hoskins et al., 1985). As pointed out by Reed (1991), the paper by Hoskins et al. "has stimulated widespread interest lately in "IPV thinking" and has lead to its application in diagnostic studies of observed cases of cyclogenesis". In the following we will show that prior to the surface development of polar low A an upper-level IPV anomaly of fairly large horizontal scale and of substantial magnitude can be observed to have advanced into the region. The development started when the upper level IPV anomaly became superimposed upon the surface "surrogate PV" (Reed, 1991) connected with surface baroclinicity along the ice-edge region and the region of strong sensible/latent heating south of Bear Island.

The use of the IPV-concept highlights the

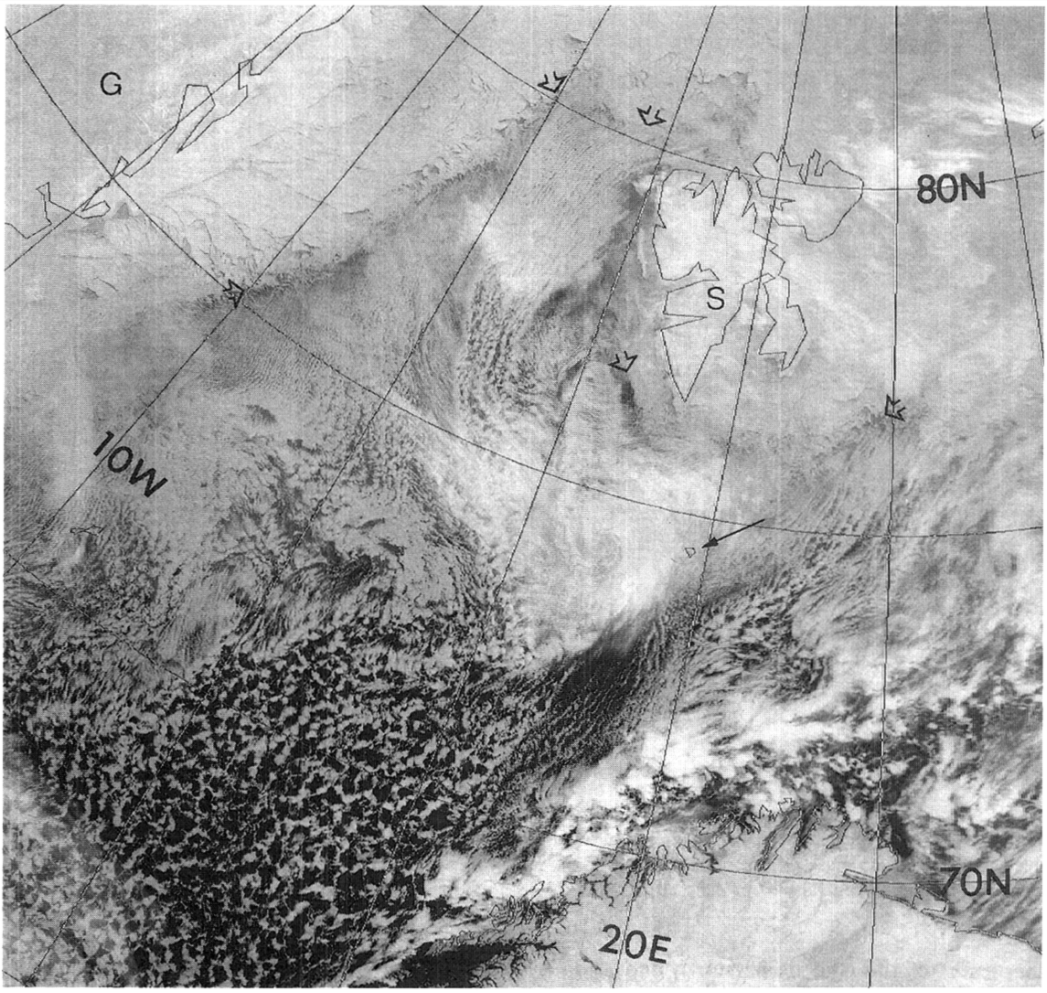

Fig. 2. NOAA-7 infrared satellite image 1257 GMT 12 December 1982 showing polar low A west of Bear Island (Bear Island marked by arrow). The ice edge around Svalbard (S) and east of Greenland (G) is indicated by open arrows. Photograph courtesy of Department of Electrical Engineering and Electronics, University of Dundee.

importance of the "solitary" upper-level disturbance and its associated vertical motion field which resulted in the cloud spiral seen on Fig. 3 at a time when neither observations nor model simulations showed any significant surface development.

2.2. The basis of the IPV analysis

To obtain the basic height and temperature fields for the IPV-analysis a 4-dimensional data assimilation was made covering the period of interest. The data assimilation was performed with the HIRLAM Level I (High Resolution Limited Area Model) system. It consists of an analysis model (essentially the ECMWF (European Center for Medium Range Weather Forecasts) scheme) and a forecast model developed by a joint Nordic/Dutch project (Machenhauer, 1988).

The data assimilation is based on a 6-h cycle using all available data from the ECMWF archive. ECMWF initialized analyses were used as boundary fields for the 6-h forecasts and the

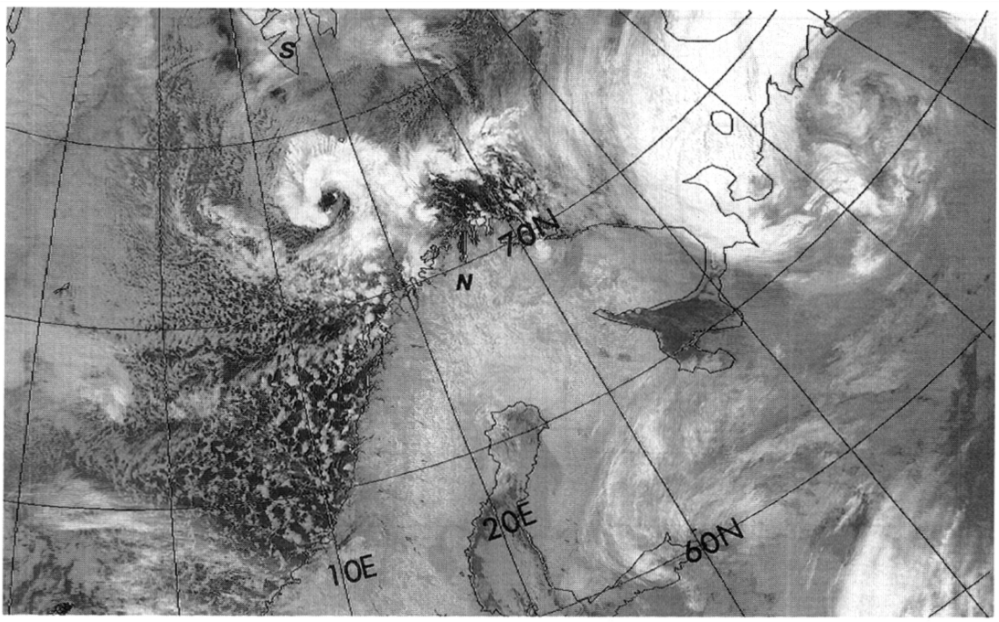

Fig. 3. NOAA-7 infrared satellite image 0250 GMT 13 December 1982 showing cloud vortex associated with the upper-level disturbance. Svalbard (S) and northern Scandinavia (N) have been indicated. Photograph courtesy of Department of Electrical Engineering and Electronics, University of Dundee.

data assimilation was initiated from the ECMWF analysis from 0000 GMT 9 December 1982. Because of the small scales involved the model must be expected to underestimate the strength of the IPV-anomalies and, to some extent, to displace the centers of the anomalies. As the sea surface temperatures and the location of the ice-border in December 1982 deviated substantially from the climatology used in the ECMWF model, these parameters were subjectively adjusted using data from the Norwegian Meteorological Institute and the US Navy.

Unfortunately the HIRLAM was not able to successfully simulate the later stages of development of the polar low, during which convective processes were of primary importance. The initial baroclinic phase of the development, however, as evidenced by observations, is fairly well represented in the assimilation and the resulting IPV analysis described below.

2.3. The IPV diagnosis

Fig. 4 shows the 290 K IPV fields in PV units (see Hoskins et al., 1985) over a 36-h period. The 290 K isentropic surface was situated below but near the tropopause level (around 350 hPa) in the Svalbard region during this period. The large positive IPV anomaly, 3 to 4 PV units, initially situated east and north-east of Svalbard at 0000 GMT 12 December 1982 is seen to have expanded horizontally while moving southward during the next 36 h. The IPV anomaly developed two local maxima during the period with one taking a southerly course towards Bear Island where it triggered the polar low development. The other maximum which followed a track north and west of Svalbard did not give rise to any development, a point we will return to later. The temperature contrasts around Svalbard between the open and partly or wholy ice covered sea, and locally low level cold air advection associated with the southward moving cold air dome as well, produced a sharp but shallow baroclinic zone near the ice-edge.

The track of the eastern of the two anomalies (EA) passed over this baroclinic zone a little southeast of Svalbard. The low level baroclinic zone close to the ice edge in this region is clearly illustrated through the temperature distribution at 1000 hPa shown on Fig. 5a. The position of the

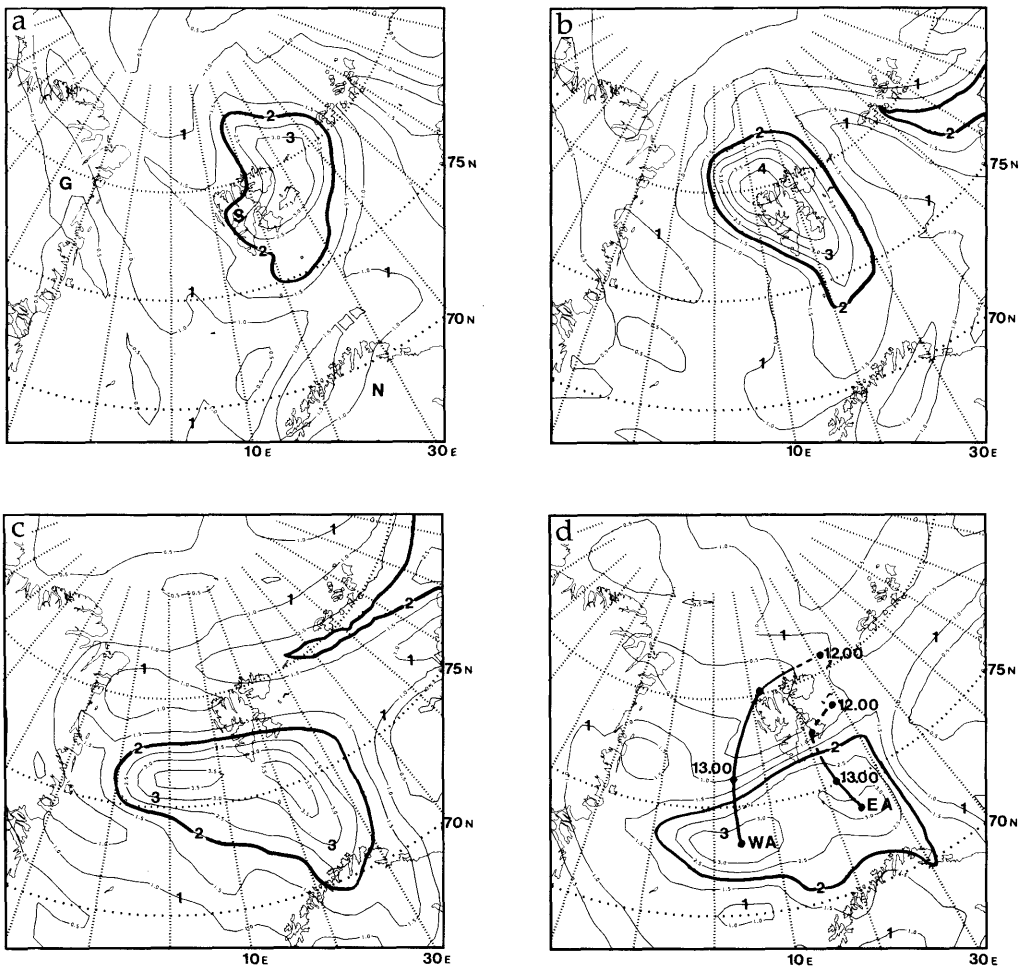

Fig. 4. Potential vorticity on the 290 K isentropic surface. Units 10^{-6} m^2 K s^{-1} kg^{-1} with the 2.0 isoline enhanced. (a) 00 GMT 12 December 1982. Greenland (G), Northern Scandinavia (N) and Svalbard (S) have been indicated. (b) 12 GMT 12 December. (c) 00 GMT 13 December. (d) 12 GMT 13 December. The tracks of the two local IPV maxima (Eastern (EA) and Western (WA)) referred to in text are shown. Stipling indicates the absence of a well-defined local maximum. Dots indicate 12-hourly positions.

baroclinic zone is clearly outlined through the region of strong horizontal temperature gradient stretching along the ice covered ocean east of Northeast Greenland over Svalbard and, further to the east along 75° N towards Novaya Zemlya. The baroclinic zone incidentally shows a striking similarity to a corresponding low level baroclinic zone discussed in a recent paper on a numerical investigation of the formation of an arctic front (Thompson and Burk, 1989, their Fig. 5b). This is so *even though the synoptic background flow in the two cases were rather different*, a fact which reflects the importance of strong local forcing for the formation of this type of fronts along the ice edge. The results of the numerical simulation by Thompson and Burk again corresponds well with aircraft observations of this particular arctic front by Shapiro et al. (1989). The well defined baroclinic zone seen along the ice edge at Fig. 5a weakens rapidly with hight but is still discernible at 855 hPa in the region southeast and east of Bear Island as shown on Fig. 5b and 5c. Fig. 5c shows the

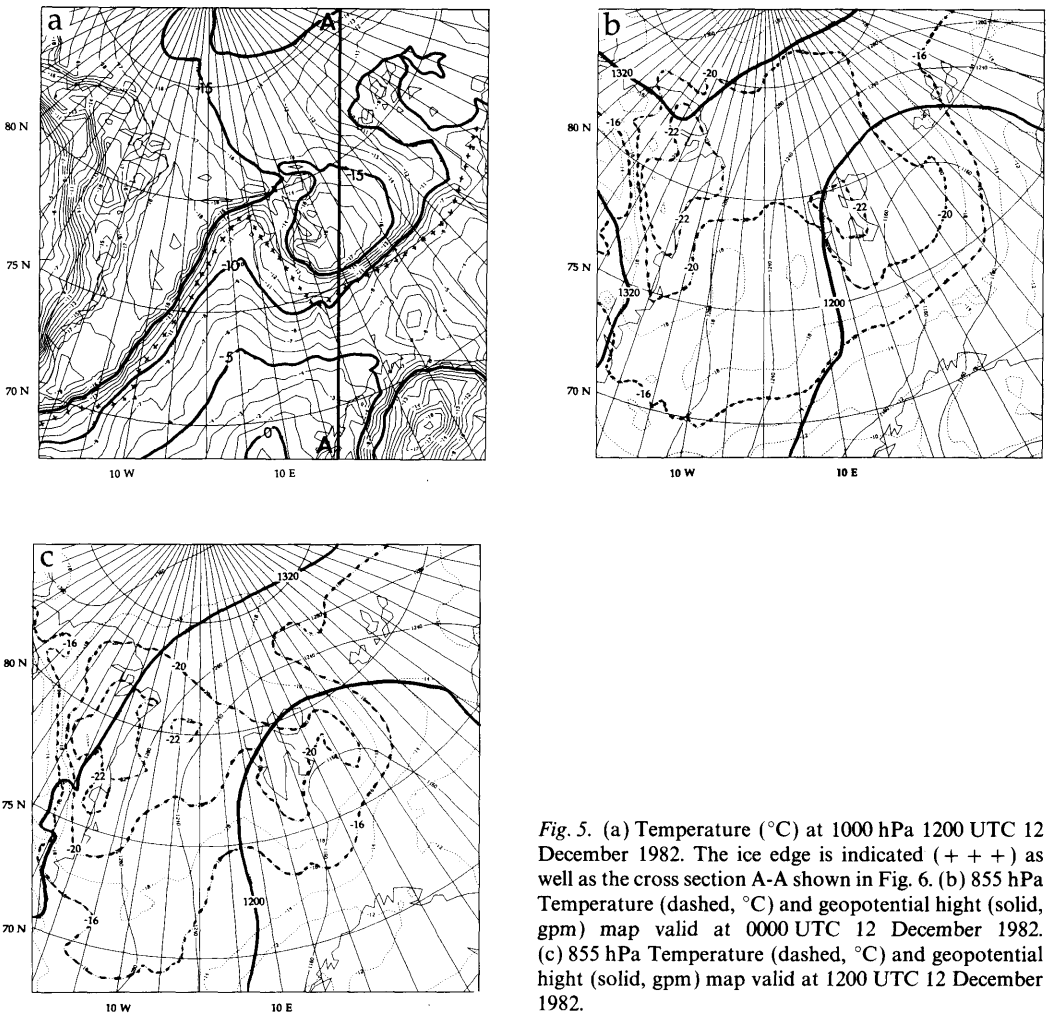

Fig. 5. (a) Temperature (°C) at 1000 hPa 1200 UTC 12 December 1982. The ice edge is indicated (+ + +) as well as the cross section A-A shown in Fig. 6. (b) 855 hPa Temperature (dashed, °C) and geopotential hight (solid, gpm) map valid at 0000 UTC 12 December 1982. (c) 855 hPa Temperature (dashed, °C) and geopotential hight (solid, gpm) map valid at 1200 UTC 12 December 1982.

situation close to the time of the initial formation of the surface disturbance. Note that the low level baroclinic zone along the ice edge south and southeast of Svalbard at this time will be intensified by cold air advection at the western side of the trough approaching the region from east. There is no indication, however, that a low level boundary front (arctic front) has formed ahead of this region of cold air advection. The structure of the low level baroclinic zone in this region is further illustrated by Fig. 6 which shows a cross section along A-A on Fig. 5a. The cross section shows that the low level baroclinic zone close to the ice edge is confined to the lowest 100 hPa or so, and that it is situated below the large synoptic scale cold dome stretching from the surface up to the 400 hPa-level.

The scenario described above bears a great resemblance to the "cyclogenesis thought experiment" of Hoskins et al., 1985 in their Subsection 6e. Following Hoskins et al., we can describe the dynamics of the first part of the development as follows: The eastern center, EA, of the upper level positive IPV anomaly moved southwards from the Svalbard region towards the ice-edge and the associated low level baroclinic zone. The low-level cyclonic circulation induced by the IPV anomaly induced a wave in the baroclinic field, which then

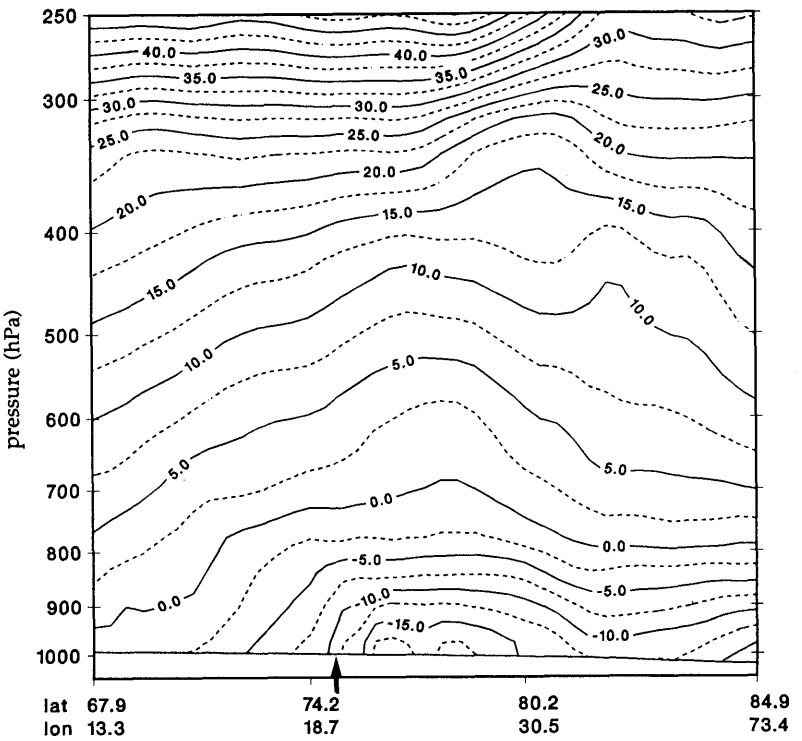

Fig. 6. Potential temperature for the cross section A-A on Fig. 5 showing the cold dome and the associated low level boundary layer (arctic) front close to the ice edge (shown by the arrow) valid at 1200 UTC 12 December 1982.

constituted a low level IPV anomaly. This low-level IPV anomaly in turn induced its own cyclonic circulation (Fig. 21, in Hoskins et al., 1985). The cyclonic flows induced by the upper and lower IPV anomalies reinforced each other and started a spin-up process. This spin-up process, however, will only be possible if the cyclonic flow induced by the upper level IPV anomaly can penetrate sufficiently deep down into the troposphere. The vertical scale for this penetration is the Rossby height (Hoskins et al., 1985) defined by

$$H = \frac{fL}{N}. \tag{1}$$

In our case, the value of the Rossby height in the vicinity of the IPV anomaly was around 5 km (for a horizontal scale of the flow, $L = 500$ km) throughout the period of interest, showing the potential for the upper level IPV anomaly to interact and participate in a spin-up process.

As a result of the baroclinic development described, a (surface) low of moderate intensity (polar low A) was formed between Bear Island and northern Norway with a central pressure around 990 hPa (see R85 Fig. 7). The horizontal scale of the low was around 500 km corresponding to the local Rossby deformation radius. Later on (see Section 3) several small-scale and quite intense disturbances developed in the region influenced by this original low.

Reed (1991) in his discussion of a case of explosive cyclogenesis notes how a positive "surrogate" IPV anomaly conducive to the production of low pressure was created near the low center by a northward advance of a tongue of warm air (a positive surface potential temperature anomaly may, according to Bretherton (1966), be regarded as a "surrogate" potential vorticity anomaly). In Reed's case, the anomaly was entirely produced by temperature advection, and air-sea interaction made no contribution to the formation

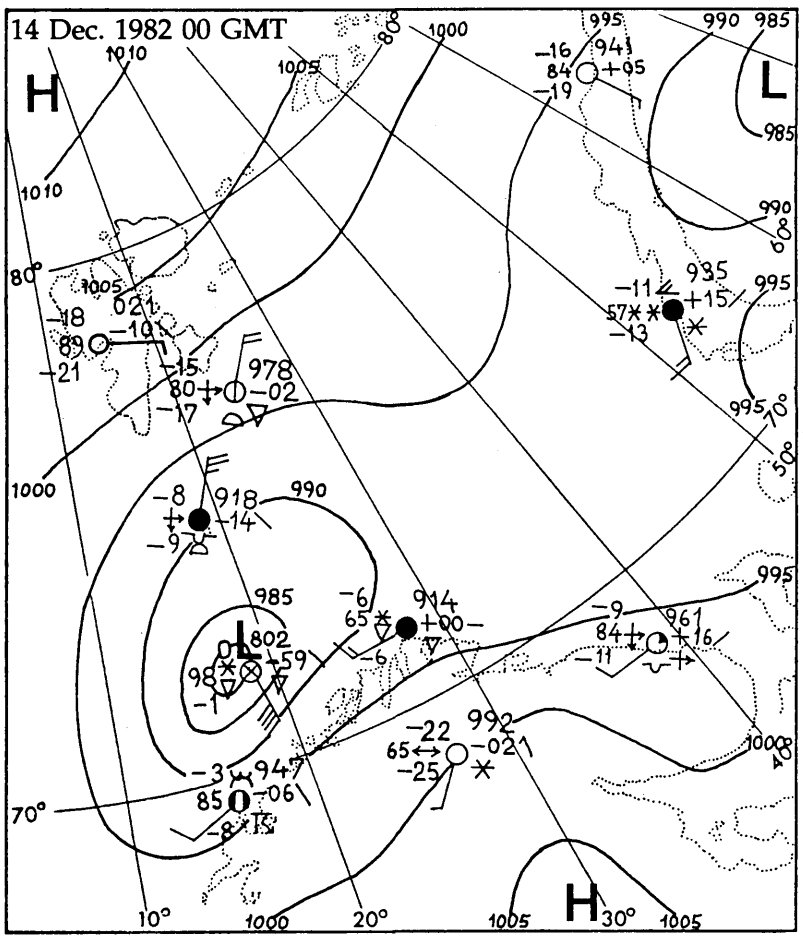

Fig. 7. Surface map 0000 GMT 14 December 1982.

of the anomaly. In the present case, both advection as well as surface heat transfer from the relatively warm sea surface south of Bear Island are bound to be important.

Upper-air IPV anomalies moving relative to the lower layers are characterized by ascent and vortex stretching ahead of the anomaly, and descent and vortex shrinking behind (Hoskins et al., 1985). In our case the upper-level IPV anomaly can be observed through the formation of the very noticiable cloud spiral (Fig. 3), before any significant development can be observed at the surface. Although baroclinic processes play an important role for the development, the cloud field in this case is strikingly different from that normally corresponding to a small baroclinic wave.

As mentioned earlier and shown on Figs. 4, actually two IPV maxima (EA and WA) moved out over the (relatively warm) sea, but only EA resulted in a polar low develoment. The western anomaly, WA, passed north, then west of Svalbard (Fig. 4d). WA did not, however, initiate any significant low-level disturbances as it entered the region free of ice between Svalbard and the north-eastern part of Greenland. The sea surface temperature in this region is fairly low and, as seen from Fig. 2, shallow and very cold air masses, originating from the surrounding ice/snow covered regions, completely covered the region down to about 70° N. From Fig. 5b and 5c it is seen that the baroclinicity at 855 hPa in the region west and southwest of Svalbard is much weaker than in the

region along the ice edge south and southeast of Bear Island. Such developments may occur in the low-level baroclinic zone along at the ice edge at the coast of Northeast Greenland, as well as further east nearer to Svalbard. However, these developments are relatively rare and almost never result in the formation of significant polar lows. There was therefore virtually no possibility in this environment for the establishment of a low-level IPV anomaly which could have led to a development corresponding to that observed further east. On the other hand polar lows sometimes do form in the "triangle" formed by Svalbard, Northeast-Greenland and 70° N.

3. The convective phase (phase two)

Between 13 December 1500 GMT and 1800 GMT, the wind at AMI increased from 10 to 15 m/s without any significant change in the surface pressure. At 1740 GMT at satellite image (not shown) showed convective cells close to the center of the synoptic scale surface low a little west of AMI. These cells were situated in a region where the sea surface temperature was as high as 8°C. Only very small pressure falls were observed at AMI prior to the increase of the wind. The convective cell observed in the central region of the low marked the starting point of the convective development leading to the formation of the subsynoptic vortex in the evening on 13 December 1982.

An intense vortex/polar low is seen on the surface maps from 14 December 0000 (Fig. 7) and 0300 GMT (the whole sequence of surface maps from the period was shown in R85). The horizontal scale of this low, as defined by the closed 990 hPa-isobar, is around 500 km, i.e., similar to the scale of the baroclinic disturbance in the preceding. An analysis of the data shows, however, that the development during this phase (phase two) was dominated by the formation of a phenomenon on a much smaller horizontal scale. Already the observations from AMI at 1800 GMT, 13 December and the satellite images from 1740 GMT and 1921 GMT indicate, that disturbances on the mesoscale were embedded in the synoptic scale circulation. In the following we will discuss this part of the development in more detail making use of satellite imagery and observations from AMI which were not available for the first part of this study reported in R85.

3.1. The convective phase of polar low A

By the beginning of phase two, when rapid pressure falls set in, the general appearance of the satellite images had undergone a dramatic change. The satellite image (Fig. 8) shows, that the synoptic scale low was in fact, at that time, a conglomerate of several subsynoptic/mesoscale phenomena, of which the most important was a tight vortex associated with the large convective cell near the center of the synoptic disturbance. Emanuel (1983) points out that "Both linear and nonlinear studies have shown that baroclinic instability has a finite horizontal scale proportional to the deformation radius NH/f, while convective and symmetric instability seek very small scales". The striking predominance of convective clouds, the small horizontal scale of the central vortex, and the rapid, localized large pressure falls all indicate that convection was the driving mechanism of polar low A during the later stages of its development. The formation of the tight vortex at the surface may be seen as the result of a rapid spin-up of vorticity associated with the pre-existing "large-scale" low due to localized deep convection in the central region of the low. A very similar mode of formation of a tight subsynoptic vortex in a homogeneous but unstable air mass was observed in the Mediterranean development discussed by Rasmussen and Zick (1987).

To represent the vertical stratification in our region of interest just prior to the start of phase 2, we may consider a "modified Bear Island sounding". Above 860 hPa this modified sounding is identical to the 1200 GMT, Bear Island sounding on 13 December (see Fig. 9). Below 860 hPa, the stable layer seen in the Bear Island sounding is replaced by a neutral layer with a constant potential temperature in order to obtain the modified sounding. The value of the (constant) potential temperature is based on the surface temperatures measured at AMI before the start of the convective development, i.e., around 271 or 272 K (see Fig. 10). The low-level neutral layer in the modified sounding was caused by strong sensible heat fluxes at the surface, and the sounding is representative of the vertical stratification just prior to the formation of the intense vortex. (Emanuel and Rotunno (1989) used a similar

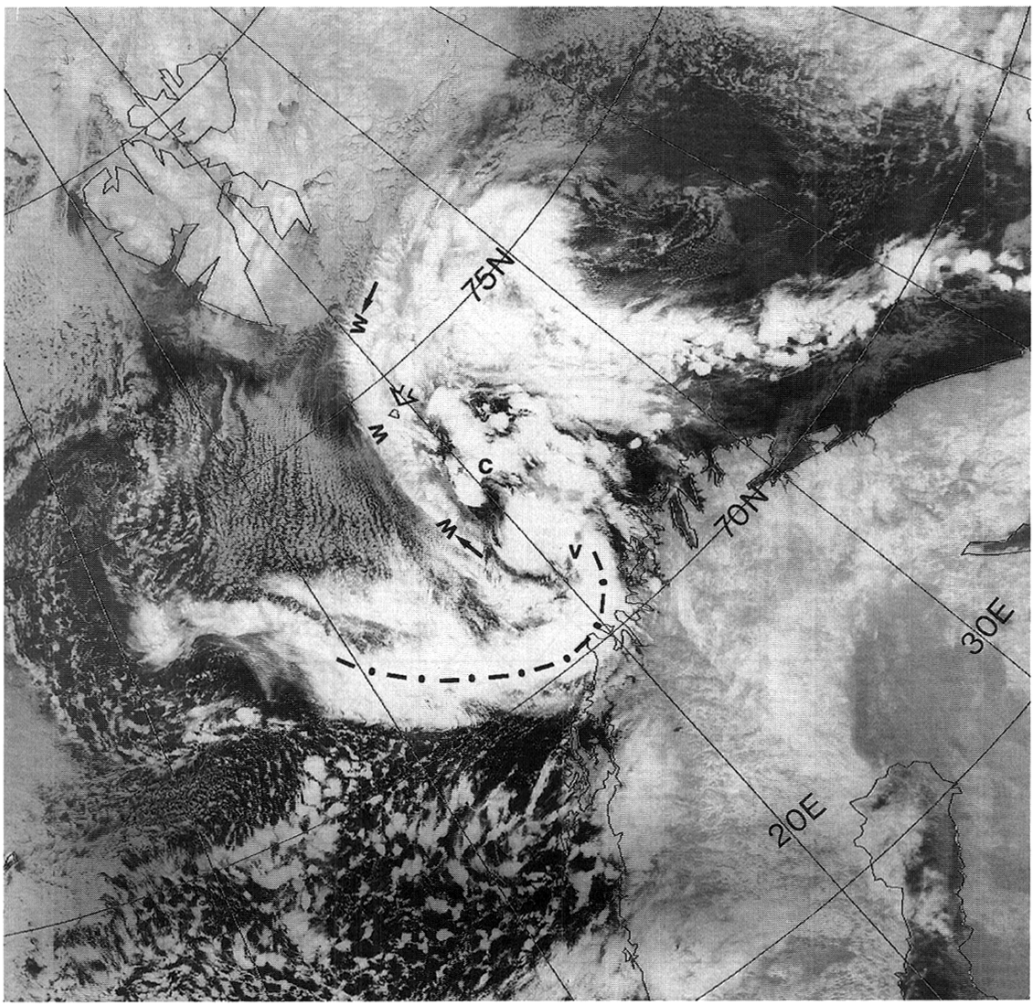

Fig. 8. NOAA-7 infrared satellite image 0419 GMT 14 December 1982. The approximate position of the center of the vortex (compare Fig. 5) has been indicated by "V". A local "arctic front" at the leading edge of the shallow cold air outbreak west of Bear Island (indicated by open arrow) is shown by the thick dash-dotted line. The shallow cold air mass can easily be identified by the system of well-developed cloud streets. The western boundary of the warm, modified air mass east of the shallow cold air mass has been indicated W-W-W. The cluster of cumulonimbus clouds marked "C", is situated in the region where vortex C is first observed around 6 h later at 1045 GMT. Photograph courtesy of Department of Electrical Engineering and Electronics, University of Dundee.

modified sounding for their "Hot, Dry-case".) During the passage of polar low A at AMI around midnight between 13 and 14 December the value of θ_w increased significantly as seen from Fig. 10. This increase was partly due to an increase in the temperature and partly to an increase in the dew point. The relatively small decrease in surface pressure (p_s) had little effect. (Ooyama, 1969) mentions that for tropical cyclones a sharp decrease in p_s may increase θ_e (and θ_w) significantly, and in this way "boost" the surface air shortly before it ascends into the warm core). The increase in the surface value of θ_w is extremely important for the potential for deep convection in the vortex. This is seen from Fig. 11 where the dashed arrow marked III shows moist adiabatic

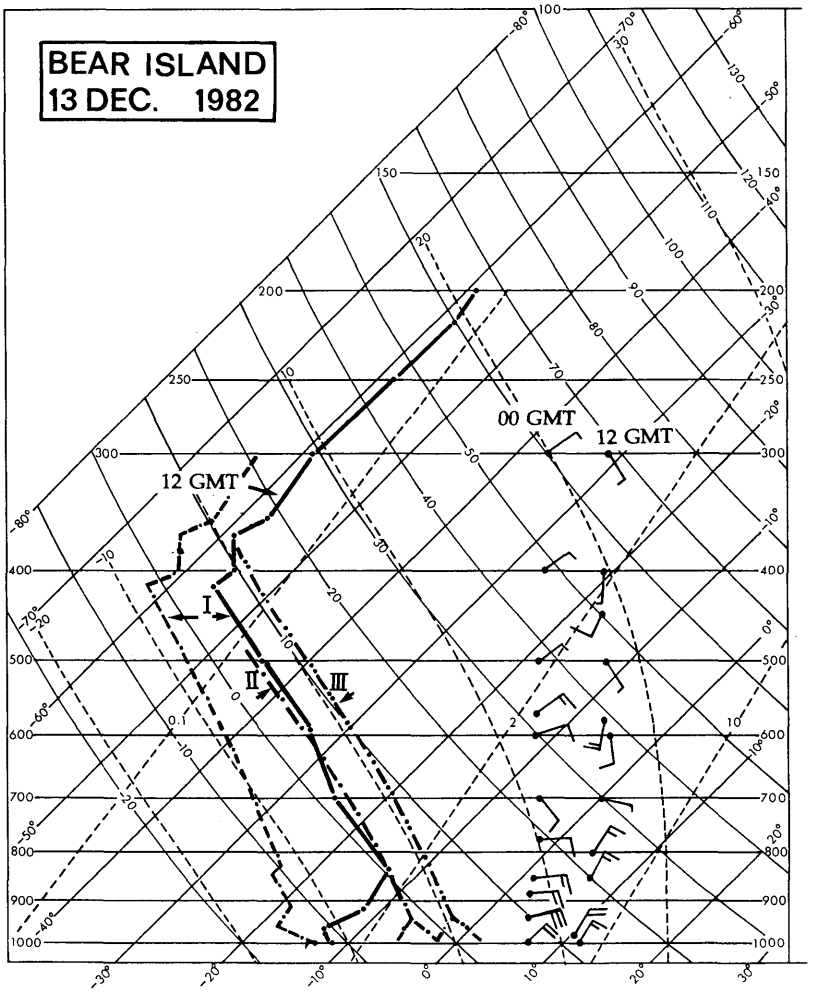

Fig. 9. Radiosonde ascent (temperature and dew-point) Bear Island 1200 GMT 13 December 1982 (curve I). Curve II shows moist adiabatic ascent of a parcel from the surface with initial temperature and dewpoint close to that measured at AMI 1200 GMT 13 December. Curve III shows moist adiabatic ascent of a parcel with a much higher surface temperature as measured later on at AMI during disturbed conditions ($\theta_w = 274$ K). The "modified" Bear Island sounding referred to in the text, is obtained by replacing the stable layer below 860 hPa with a neutral layer $\theta = 272$ K. Winds are given with north "upwards" and long barbs indicate 5 m/s.

ascent from the surface corresponding to the maximum θ_w value (274 K) measured at AMI during the passage of the polar low. The dashed arrow II correspondingly shows moist adiabatic ascent from the surface starting at 271 K representative of the conditions away from the polar low. Following Ooyama θ_w^* corresponds to the potential wet bulb temperature assuming that the air is saturated at each level.

By integrating the hydrostatic equation from the surface to H, the level of the tropopause, we find the following expression for the surface pressure decrement Δp_0 at the surface due to an increase $\Delta \bar{T}$ in the mean temperature.

$$\Delta p_0 = -\frac{gHp_0\,\Delta \bar{T}}{R\bar{T}^2} \simeq 4\,\Delta \bar{T}. \qquad (2)$$

Anthes (1982, pp. 74–75) has pointed out, that a warm core may be formed through the replace-

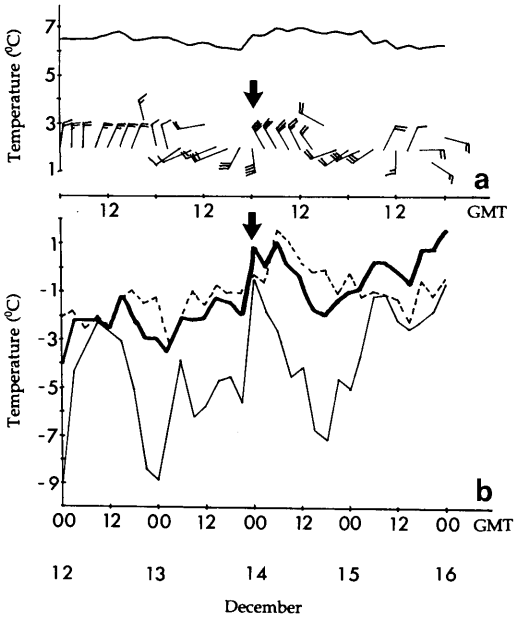

Fig. 10. Observations from weathership AMI. The arrow shows the time at which the center of vortex A passes AMI. (a) Surface winds in m/s (long barb indicates five m/s) and north "upwards". Sea surface temperature (thin solid line). (b) Surface air temperature (thin dashed line), dewpoint temperature (thin solid line), surface wet bulb potential temperature (θ_w, thick solid line).

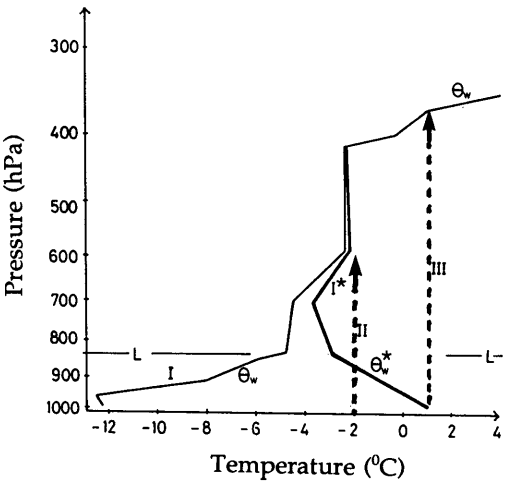

Fig. 11. Stratification of fresh arctic air (curve I) shown by the wet bulb potential temperature θ_w. The thick curve marked I* shows θ_w^* corresponding to the modified Bear Island ascent obtained by replacing the temperature below level L at 830 hPa with a dry adiabatic layer. See text for definition of θ_w^*. The vertical dashed lines II and III describe moist adiabatic ascent from the surface with θ_w equal to respectively −2°C and 1°C.

ment of an unsaturated column of air with a cloud of higher mean temperature, and that this mechanism is among three which may be responsible for the tropospheric warming necessary to produce a hurricane from a weak disturbance. The satellite image, Fig. 8, shows deep and widespread convection in the central region of the polar low centered at "V". Assuming, following Anthes, that a column of relatively high temperature is formed due to the convection, we may compute the resulting surface pressure deficit through eq. (2) provided an estimate can be found for $\Delta\bar{T}$. A maximum value for $\Delta\bar{T}$ (and for the corresponding pressure fall Δp_0) can be obtained by assuming moist adiabatic ascent from the surface corresponding to the highest θ_w measured at AMI during the passage of the polar low (see Fig. 10 and curve III Fig. 9). Inspection of Fig. 9 shows, that for this case $\Delta\bar{T} \simeq 3.5$°C which corresponds to a maximum surface pressure decrement of $\Delta p_0 \simeq$ 14 hPa. Based on observations at AMI, the actual surface pressure disturbance associated with polar low A is around 10 hPa which indicates a slightly smaller mean temperature in the central region of the low than that corresponding to undiluted moist adiabatic ascent.

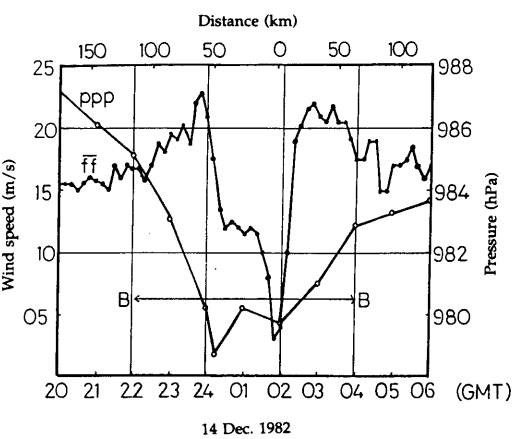

Fig. 12. Mean wind velocity (ff) in m/s (10 minutes mean) and surface pressure (ppp) from weathership AMI (71.5°N, 19°E) from 2000 GMT 13 December 1982 to 0600 GMT 14 December 1982.

Tellus A/44/2-5

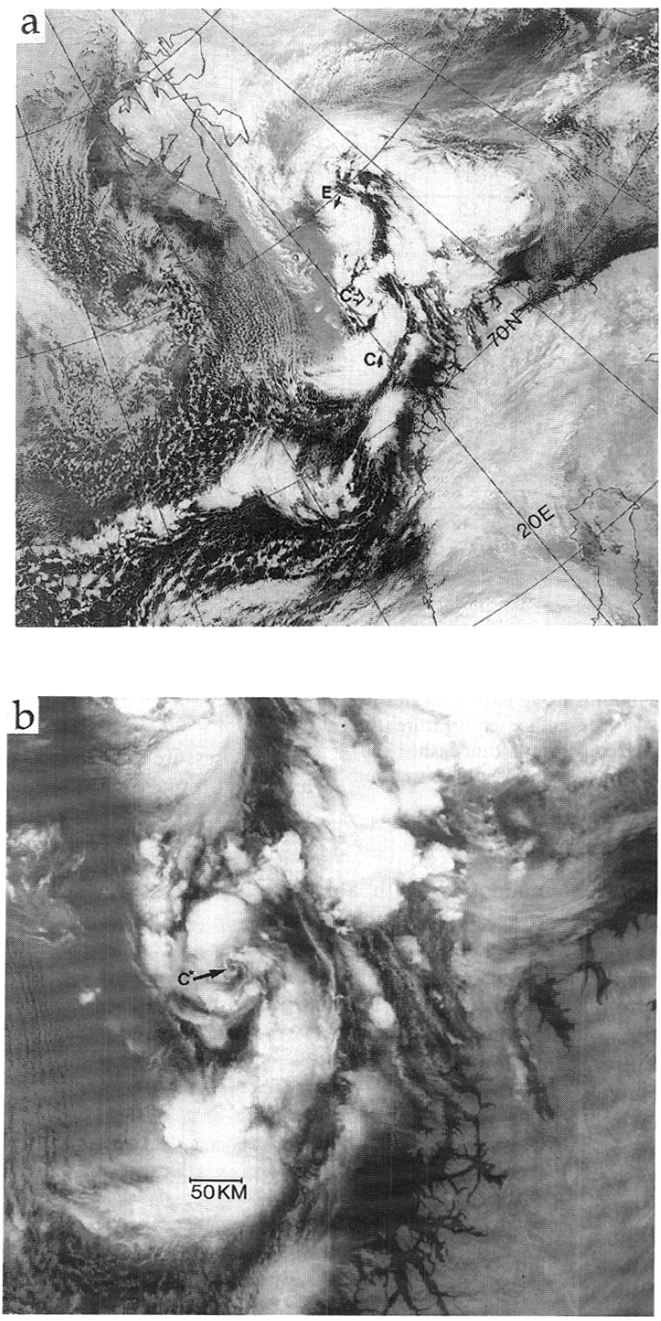

Fig. 13. (a) NOAA-7 infrared satellite image 0406 GMT 15 December 1982. Arrows marked C, C* and E show the decaying vortex C, the newly formed vortex C* and the cumulonimbus cluster which later on developed into vortex E. The shallow cold air mass east of 20° E is clearly indicated by the system of cloud streets and the region of a shallow overcast. (b) An enlargement of the region around vortex C* in Fig. 13a. Photograph courtesy of Department of Electrical Engineering and Electronics, University of Dundee.

After the initial formation of the vortex a little west of AMI, it moved in an east to south-easterly direction and the central region passed just over or very close to AMI. The mean wind velocity and pressure as function of time during the passage of the center are shown in Fig. 12. By means of the observed translation velocity of the vortex we can transform the time-axis into the equivalent length scale also shown on the figure. The distance between the wind-maxima on Fig. 12 is seen to be only around 100 km. The asymmetry of the wind velocity and the pressure distribution illustrate what can actually be inferred from satellite images (not shown) that at least two mesoscale vortices existed in the central region of the vortex.

The mean values of the wind velocity (10 minute mean-values) shown in Fig. 12 reach about 23 m/s. The instantaneous values and the wind directions are missing (except at the three-hourly synoptimes). Based on measurements from a similar vortex passing Bear Island on 15 December 1982 (see Subsection 3.2) we may assume, that the wind velocity in the (frequent) gusts have reached values as high as 40 m/s.

Based on the variation of the surface pressure at AMI, we might define the horizontal scale for the vortex by B-B shown on Fig. 12. This corresponds to a horizontal scale around 175 km.

*3.2. The formation and development of arctic instability lows C and C**

After the spin-up process in the central region of the previously formed low, the resulting vortex (vortex A) can be followed for about 18 h. Beginning around 14 December 1045 GMT, another subsynoptic disturbance, low C, developed around 73°N, 21°E, close to a cluster of cumulonimbus clouds already discernible at 0419 GMT (see Fig. 8), and close to the front W-W-W, also shown in Fig. 8.

A close inspection of the satellite image from 1227 GMT, 14 December reproduced in R85 as Fig. 6 shows, that the central part of low C consisted of a mesoscale vortex of a horizontal scale less than 100 km, including a diminutive eye appearing as a black dot. In R85 Fig. 3, it is shown that the trajectory of low C made a small loop between 14 and 15 December. A closer analysis has revealed, however, that this is not true. Instead a new vortex, C* (see Fig. 13a), formed very close to C around midnight and rapidly took over as the dominant one, while the "old" vortex C moved further southwards under decay. C as well as C* are true mesoscale phenomena with a horizontal scale even less than that of vortex A. Nevertheless they show a well defined horizontal structure with diminutive eye-like features. Like C, C* formed in a region of vigorous convection close to the boundary between the shallow cold air to the west and the warmer unstable airmass to the east. In Fig. 13a, we can actually observe a whole "polar low-family" along the shallow arctic frontal zone analogous to the well known extratropical cyclone-family, with C decaying, C* in its mature phase, and E in its developing phase.

The cloud streets west and southwest of Bear Island (see Fig. 13a) indicate a strong local outbreak of a shallow cold air mass and the

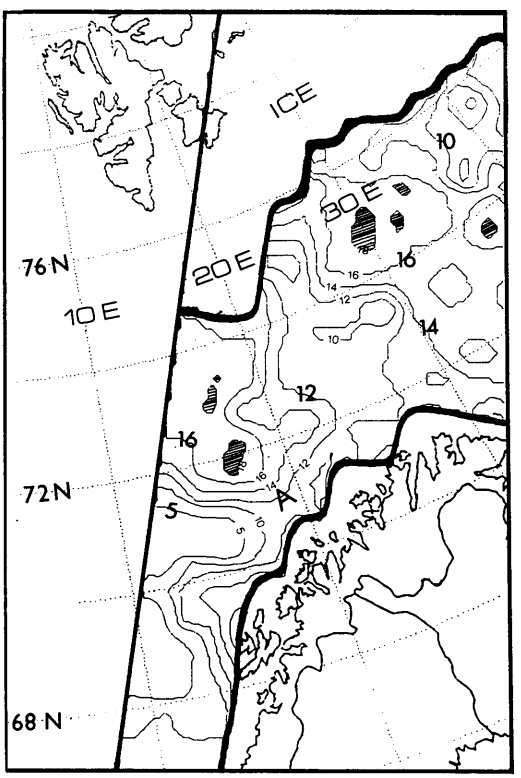

Fig. 14. SMMR-derived surface wind velocities (m/s) 0013 GMT 15 December 1982. Isotachs drawn for 5 m/s, 10 m/s and then every 2 m/s. Hatched areas indicate wind velocities greater than 18 m/s. Weather ship AMI is indicated by "A".

orientation of the streets shows the approximate wind direction. Additional information about the strength of the outbreak is shown in Fig. 14. This figure shows the surface wind velocity close to the time of the satellite image, i.e., at 0013 GMT, 15 December. The hatched areas represent velocities more than 18 m/s, and two such maxima can be seen in the region south-southwest of Bear Island.

The surface wind velocity shown were obtained from the Scanning Multichannel Microwave Radiometer (SMMR) abord the Nimbus-7 satellite. In order to get the best possible spatial resolution (30 km) the algorithm used for the determination of the wind speed was based on the 0.8 cm wavelength (37 GHz) only. Including one or both 1.7 cm channels would have reduced the horizontal resolution to 60 km which was considered too coarse for the present study. Such an algorithm was not available in the literature and had to be developed specially for this purpose. The method for deriving the algorithm was to make use of a stepwise linear regression between a set of observed winds and corresponding Nimbus-7 measurements (within 50 km and one hour) at weather ship MIKE (66°N, 02°E) in the Norwegian Sea close to the region of development of the polar low. The wind algorithm reads

$$WS(\mathrm{m/s}) = 254.3 + 1.298T_B(0.8H) - 2.219T_B(0.8V),$$

where $T_B(0.8H)$ and $T_B(0.8V)$ respectively is the horizontally and vertically polarized brightness temperatures at wavelength 0.8 cm. The SMMR surface wind velocities derived in this way are in good qualitatively agreement with the observed surface wind velocities in the region.

Fig. 13b shows an enlargement of vortex C*. The center or the "eye" is clearly discernible and the orientation of the low-level cloudbands indicate a fairly symmetric low level cyclonic circulation. The clouds associated with the vortex are mostly low-level clouds except from the big cumulonimbus seen north of the center. The vortex is definitely of smaller horizontal scale than that normally associated with polar lows. The term arctic instability low has sometimes although not very often been used synonymously with polar lows. The use of "instability" implies that convection is active and the term may be a good alternative name for those kinds of very small vortices, convective in nature. Such vortices have not so far been discussed in the literature. Økland (1987) suggested that the circulation in some polar lows might consist of two different scales, in the way that a mesoscale circulation was embedded in a vortex of a somewhat larger dimension. Økland presents an example of a small scale vortex embedded in a larger cyclonic circulation, a case which has some similarities to the one discussed here.

The center of C* fortuitously passed very close to Bear Island around 1500 GMT 15 December 1982. Fig. 15 shows the instantaneous surface wind velocity, and Fig. 16 the surface pressure during the passage of C*. Fig. 17 shows the 10-min mean wind and the surface pressure together. The wind field revealed by these measurements in many ways is similar to the wind fields associated with vortex A (compare Figs. 12 and 17), although it is a little more symmetric. The velocity, however, is somewhat weaker. Provided the wind is caused by an (approximately) axisymmetric vortex (as indicated by Fig. 13b) the wind shows an almost linear variation from the center where the velocity is very

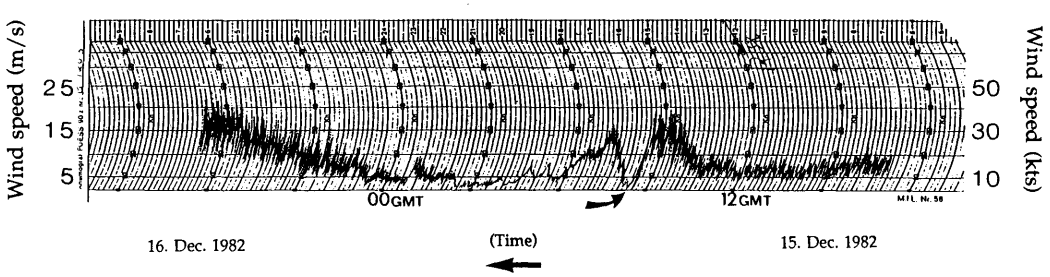

Fig. 15. Surface observation from Bear Island during the passage of vortex C* showing wind velocity in knots. The passage of the "eye" has been marked by an arrow. Time is given in local time, i.e., GMT plus one hour.

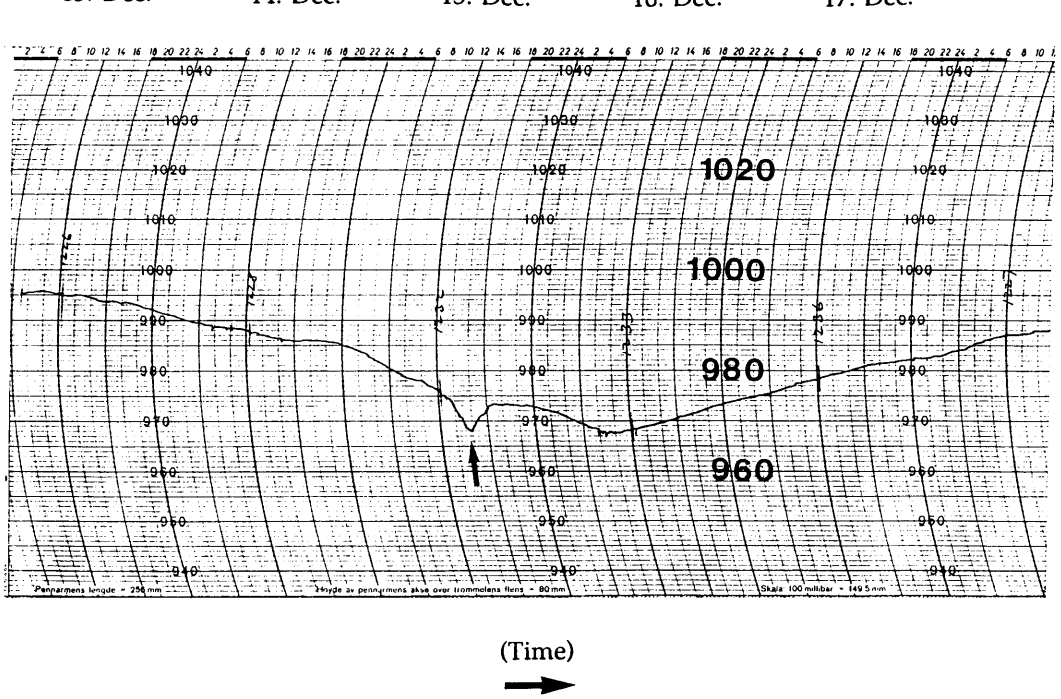

Fig. 16. Barograph record from Bear Island showing surface pressure from 0600 GMT 13 December to 18 December 1982.

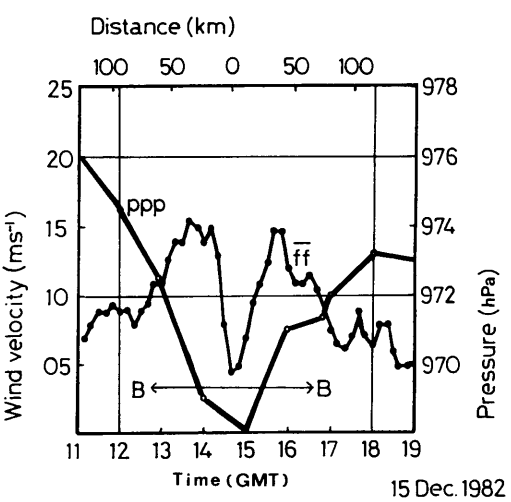

Fig. 17. Mean surface wind velocity (ff) in m/s (10 minutes mean) and surface pressure (ppp) from Bear Island 1100 GMT to 1900 GMT, 15 December 1982.

small to the region of maximum velocity around 35 km away, corresponding to a core in solid rotation. (It is not possible of course, based on observations from Bear Island alone to decide whether the observed wind changes are caused by a vortex or by for example a shear line. Satellite images as Fig. 13 do indicate, however, that the disturbance is approximately axisymmetric at last in lower levels). The wind was very gusty and the ratio between the peak gust values and the mean wind is around 1.5 or a little higher. Altogether the measurements reveal a tight, symmetric vortex of "medium" intensity and of a small horizontal scale around 150 km corresponding to B-B on Fig. 17. Note that the horizontal distance between the wind maxima is only around 75 km. Using the values of Δp and r corresponding to the distance from the center to the radius of maximum mean wind, i.e., $\Delta p \simeq 3$ hPa and $r = 35$ km, we find that the gradient wind, is $\simeq 13$ m/s, in agreement with the observed wind. This fact together with other

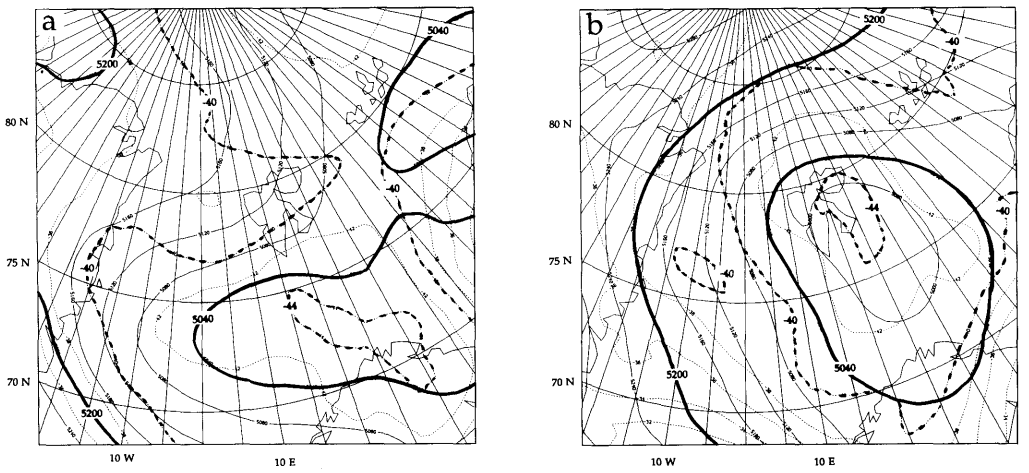

Fig. 18. (a) 500 hPa map 1200 UTC 12 December 1982. (b) 500 hPa map 1200 UTC 13 December 1982. Solid line shows hights in intervals of 40 gpm, and the dotted lines temperatures in intervals of 2°C. The position of weater ship AMI is indicated on the maps.

evidence indicate that balanced motion indeed occurred even at these very small horizontal scales and over a considerable time period as well. To explain this we must bear in mind that the mesoscale vortex developments took place in an already existing vortex of somewhat larger dimension (radius $R \simeq 250$ km). In this case following Ooyama (1982) and Frank (1983), the Rossby radius $\lambda = ND/f$ should be replaced by a local Rossby radius, R_0, given by

$$R_0 = \frac{ND}{(\xi + f)^{1/2}(2V/R + f)^{1/2}},$$

in order to take into account the influence of the rotating flow. N is the Brunt-Väisälä frequency, D the depth of the (active) convection and V the velocity at the distance R. Using (based on observations) $N = 0.7 \times 10^{-2}\,\mathrm{s}^{-1}$ (corresponding to an approximate moist adiabatic stratification), $V = 20$ m/s, $R = 250$ km, and an estimated value of $D = 4000$ m, we find that $R_0 = 80$ km as compared to the much larger value $\lambda = 400$ km valid for the corresponding non-rotating atmosphere. According to Ooyama, disturbances on a horizontal scale larger than local Rossby radius are dynamically large and may be assumed to be balanced. The low value of the local radius of deformation in our particular case therefore explains why balanced disturbances of small horizontal scale can exist over long time intervals. On the other hand, again following Ooyama (1969), very small disturbances cannot grow because of internal friction.

3.3. *Upper air-conditions and final development*

As already mentioned, the polar low developments on 13 and 14 December took place within the central region of a large synoptic scale cold dome moving in a southerly direction over our region of interest. The extension of the cold dome and its movement may be seen from the temperature distribution at the 500 hPa level illustrated in Fig. 18a and 18b. At the time of the first (baroclinic) polar low development early on 12 December the center of the cold air at the 500 hPa level is found somewhat north to northeast of the region of the incipient polar low development. On the evening of 13 December, when the convective development was first observed, the center (and coldest part) of the synoptic scale cold air dome was situated right over the region of development.

The NOAA-7 infrared satellite image from 1400 GMT 15 December 1982 reproduced as Fig. 19 shows a continued asymmetric structure of the cloud field associated with vortex C*, the high

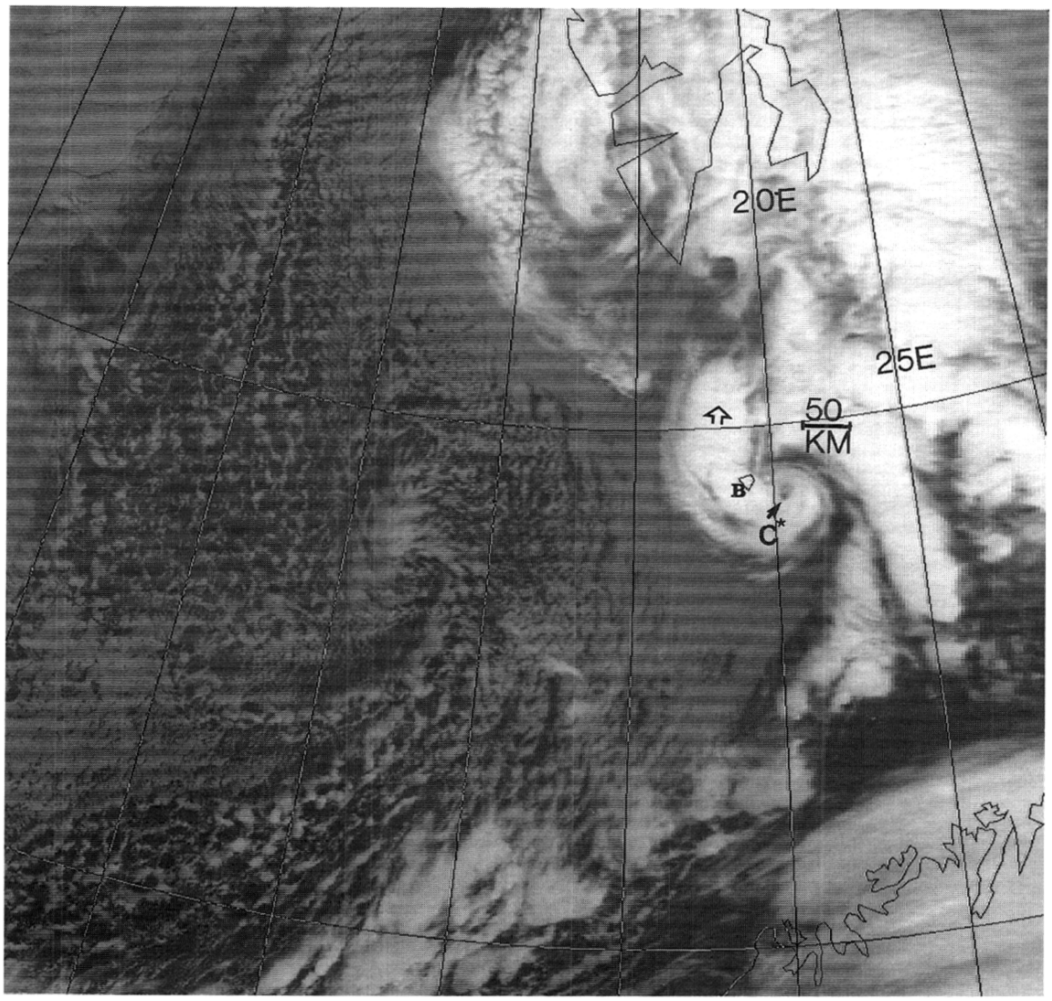

Fig. 19. NOAA-7 infrared image 1400 GMT 15 December 1982 showing vortex C* east of Bear Island (marked by B). The open arrow indicates the upper level outflow. Photograph courtesy of Department of Electrical Engineering and Electronics, University of Dundee.

clouds over or near Bear Island still being situated away from (west of) the center. Bear Island at this time was still covered by the shallow cold air mass clearly indicated on the radiosonde ascent from 1200 GMT (not shown), and any deep convection to the west (of Bear Island) must have been due to forced ascent of warmer air from the east, up above the shallow cold air mass. In this way the deepest convection becomes decoupled from the central parts of the vortex.

Low C* can, as already mentioned, first be observed on the satellite images around midnight between 14 and 15 December. From the 500 hPa-map from 0000 GMT, 15 December 1982 (not shown) it is seen that the initial formation of C* took place below an upper-level (cold) vortex. Vortex C* can, by means of satellite images, be followed on its track westwards until it finally decays after "icefall" on the pack-ice at the coast of Northeast Greenland on 16 December. Fig. 20 shows vortex C* before the icefall at 0354 GMT 16 December. Compared to 1400 GMT 15 December

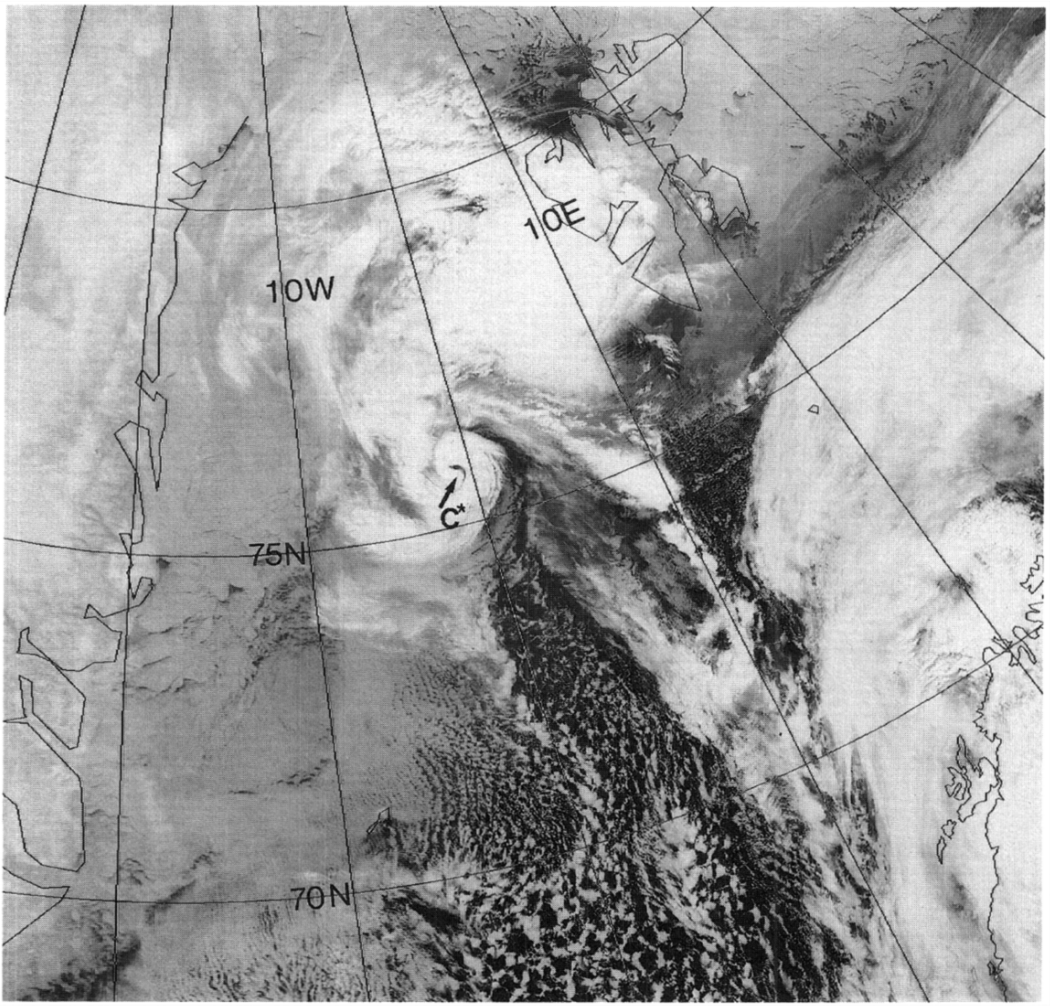

Fig. 20. NOAA-7 infrared satellite image 0354 GMT 16 December 1982 showing vortex C*. Photograph courtesy of Department of Electrical Engineering and Electronics, University of Dundee.

(Fig. 19) the structure had changed considerably and at this time resembled a baroclinic system of very small scale. The high level cirrus were wrapped around the center and at low levels cold air from the pack ice has been drawn into the circulation.

4. Summary

In Rasmussen (1985) and in the present work, we have carried out a study of an unusually long "polar low episode" of about 4 days duration over the Barents Sea, the northern part of the Norwegian Sea and the East Greenland Sea. The study has revealed that many phenomena and mechanisms interact in a complex way to create circulation systems on widely different horizontal scales. The region with its varied and unique geography makes it possible for very cold air with surface temperatures below $-20°C$ to flow directly out over a relatively warm sea with surface temperatures of 5°C or even more. Along the ice edge secondary baroclinic zones are often

observed and the shallow cold air outbreaks sometimes are headed by arctic fronts. These factors as well as others, mean that a variety of atmospheric forcing mechanisms are possible including CISK (Conditional Instability of the Second Kind) and baroclinic instability, which can give raise to a whole spectrum of disturbances.

As discussed in R85, the episode was initiated by an upper-level cold core vortex. Upon crossing the ice edge near Svalbard early on 12 December 1982, the upper-level vortex triggered a surface disturbance of baroclinic nature, and of a horizontal scale corresponding to the Rossby deformation radius of $\lambda \simeq 400$ km. Qualitative arguments based on the omega equation and "IPV thinking" support the point of view that the initial development is of baroclinic nature.

The baroclinic development on 12 and 13 December 1982 as well as the convective developments on 13, 14 and 15 December *all* take place within a large synoptic scale cold dome (Figs. 6, 18). The formation of the low level baroclinic zone which is of crucial importance for the ensuing developments may be ascribed partly to strong differential heat fluxes along the ice edge, *but to low level cold air advection connected with the advance of the synoptic scale cold dome as well.* Later on, the convective disturbances develop in the central region of the cold dome, i.e., in the region with very low temperatures aloft, promoting deep convection. The cold dome in this way is equally important for the initial formation by providing and/or enhancing an already existing low level baroclinic zone, as well as later on when deep convection develops in the central region of the cold dome. This dual function of cold air domes has been observed elsewhere as for example in connection with polar low formations over the Labrador Sea. A particular well documented case of a Labrador polar low formation is discussed by Rasmussen and Purdom (1992). It therefore seems, that *the formation of a large subgroup of polar lows, including baroclinic as well as "convective" disturbances, can be explained as the result of processes connected with the advance of synoptic scale cold domes from the interior snow/ice covered regions, across the ice edge, out over relatively warm ocean regions.*

During the southward movement, the air became increasingly modified, a neutral or unstable lapse rate developed in the lower layers and convection became increasingly important. This development culminated in the evening on 13 December when an intense vortex was formed through a rapid spin-up process near weather ship AMI. The central part of the vortex passed over AMI and observations from the ship show, that the pressure perturbation associated with the newly formed vortex was around 10 hPa.

This corresponds approximately to the expected hydrostatic pressure deficit in a region of saturated ascent by surface air with properties as observed at AMI. The horizontal scale of the vortex was significantly smaller than that of the first formed baroclinic low. In the next two days several vortices of a surprisingly small horizontal scale were formed in the modified "warm" air mass, all close to its western flank and to the shallow cold arctic air mass farther west.

Vortices of this kind have seldom if ever been studied in detail before. As discussed in the previous sections the center of one of these vortices, C*, passed over Bear Island. The observations on that occasion showed a disturbance of moderate intensity. The wind field (assuming radial symmetry) was roughly in gradient balance and the corresponding pressure disturbance was quite small.

The formation of vortices like C and C* can hardly be explained alone in terms of exceptional, local deep convection in the unstable air mass. A more plausible explanation is that the convective vortices are modulated by low-level baroclinic instability, associated with the shallow frontal zone at the western flank of the warm, modified unstable air-mass. Theoretical results (Blumen, 1979; Wiin-Nielsen, 1989) do show, that baroclinic disturbances of a very short wavelength can form in such conditions. The small horizontal scale of the vortices and the fact that they all form close to the western flank of the region of deep convection, indicate that such a mechanism may be at work. Since very shallow outbreaks of arctic air over a relatively warm sea surface are specific for the region considered, this may be the explanation why mesoscale vortices like C* have not been observed elsewhere before.

5. Acknowledgments

The authors thank Magne Lystad, The Norwegian Meteorological Institute for making

data available for this study. We also thank Dr. Michael W. Douglas, University of Colorado for providing Fig. 1 from the DMSP archive and the HIRLAM-group for assistance and use of their model. Finally we thank Dr. Stephen Smith, CIRA, Colorado State University for reading the manuscript and for many useful comments and Charlotte Autzen, The Danish Meteorological Institute, for preparing figures. Part of the work was carried out under Office of Naval Research Grant N00014-87-G-0232, and partly supported by the Greenland Sea Project (GSP).

REFERENCES

Anthes, R. A. 1982. Tropical cyclones. Their evolution, structure and effects. *Meteorological Monograms, 19*, American Meteorological Society.

Blumen, W. 1979. On Short-wave baroclinic instability. *J. Atmos. Sci. 36*, 1925–1933.

Bretherton, F. P. 1966. Critical layer instability in baroclinic flows. *Quart. J. Roy. Meteor. Soc. 92*, 325–334.

Businger, S. 1985. The synoptic climatology of polar low outbreaks. *Tellus 37A*, 419–432.

Emanuel, K. A. 1983. On the dynamical definition(s) of "mesoscale". In: *Mesoscale meteorology-theory, observations and models* (eds. D. K. Lilly and T. Gal-Chen). Dordrecht-Boston, D. Reidel Publishing Co., 1–11.

Emanuel, K. A. and Rotunno, R. 1989. Polar lows as arctic hurricanes. *Tellus 41A*, 1–17.

Frank, W. M. 1983. The cumulus parameterization problem. *Mon. Wea. Rev. 111*, 1859–1871.

Hoskins, B., McIntyre, M. E. and Robertson, A. W. 1985. On the use and significance of isentropic potential vorticity maps. *Quart. J. Roy. Meteorol. Soc. 111*, 877–946.

Eliassen, A. and Kleinschmidt, E. 1957. *Dynamic meteorology*. Handbuch der Physik, Springer Verlag, 1–154.

Machenhauer, B., (Ed.). 1988. HIRLAM Final Report. *HIRLAM Technical Report no. 5*, Copenhagen December 1988, 116 pp. Available from the Danish Meteorological Institute, Lyngbyvej 100, DK-2100 Copenhagen Ø, Denmark.

Nordeng, T-E. and Rasmussen, E. 1992. A most beautiful polar low. A case study of a polar low development in the Bear Island region. *Tellus 44A*, 81–99.

Økland, H. 1987. Heating by organized convection as a source of polar low intensification. *Tellus 39A*, 397–407.

Ooyama, K. V. 1969. Numerical Simulation of the life cycle of tropical cyclones. *J. Atmos. Sci. 26*, 3–40.

Ooyama, K. V. 1982. Conceptual evolution of the theory and modelling of the tropical cyclone. *J. Meteorol. Soc. Japan 60*, 369–379.

Rasmussen, E. 1985. A case study of a polar low development over the Barents Sea. *Tellus 37A*, 407–418.

Rasmussen, E. and Lystad, M. 1987. The Norwegian Polar Lows Project: A summary of the *International Conference on Polar Lows, 20–23 May 1986*, Oslo, Norway. Bull. Amer. Meteorol. Soc. 68, 801–816.

Rasmussen, E. and Purdom, J. F. 1992. A multisatellite investigation of a polar low development over the Labrador Sea. *6th Conference on Satellite Meteorology and Oceanography*, 5–10 January 1992, Atlanta. American Meteorological Society.

Rasmussen, E. and Zick, C. 1987. A subsynoptic vortex over the Mediterranean with some resemblance to polar lows. *Tellus 39A*, 408–425.

Reed, R. J. 1979. Cyclogenesis in polar airstreams. *Mon. Wea. Rev. 107*, 38–52.

Reed, R. J. 1986. Baroclinic instability as a mechanism for polar low formation. Proceedings of *The International Conference on Polar Lows*, Oslo, Norway, 20–23 May 1986, 364 pp. Available from the Norwegian Meteorological Institute.

Reed, R. J. 1991. Cyclogenesis from a potential vorticity perspective. Preprints from *1st International Symposium on Winter Storms*, New Orleans, LA. 14–18 January 1991, 436 pp. American Meteorological Society.

Thompson, W. T. and Burk, S. D. 1989. An investigation of an arctic front with a vertically nested mesoscale model. *Mon. Wea. Rev. 119*, 233–261.

Shapiro, M. A., Hampel, T. and Fedor, L. S. 1989. Research aircraft observations of an arctic front over the Barents Sea. In: *Polar and arctic lows* (ed. P. F. Twitchell, E. A. Rasmussen and K. L. Davidson). A Deepak Publishing, Virginia, USA, 420 pp.

Wiin-Nielsen, A. 1989. On the precursors of polar lows. In: *Polar and arctic lows* (ed. P. F. Twitchell, E. A. Rasmussen and K. L. Davidson). A Deepak Publishing, Virginia, USA, 420 pp.